

A Freestanding Stretchable and Multifunctional Transistor with Intrinsic Self-Healing Properties of all Device Components

Muhammad Khatib, Tan-Phat Huynh, Yunfeng Deng, Yehu David Horev, Walaa Saliba, Weiwei Wu, and Hossam Haick*

A flexible and stretchable field-effect transistor (FET) is an essential element in a number of modern electronics. To realize the potential of this device in harsh real-world conditions and to extend its application spectrum, new functionalities are needed to be introduced into the device. Here, solution-processable elements based on carbon nanotubes that empower flexible and stretchable FET with high hole-mobility ($\mu_h \approx 10 \text{ cm}^2 \text{ V}^{-1} \text{ s}^{-1}$) and relatively low operating voltages ($<8 \text{ V}$) and that retain self-healing properties of all FET components are reported. The device has repeatable intrinsic and autonomic self-healing ability, namely without use of any external trigger, enabling the restoration of its electrical and mechanical properties, both after microscale damage or complete cut of the device—for example by a scissor. The device can be repeatedly stretched for >200 cycles of up to 50% strain without a significant loss in its electrical properties. The device is applicable in the form of a $\approx 3 \text{ }\mu\text{m}$ thick freestanding skin tattoo and has multifunctional sensing properties, such as detection of temperature and humidity. With this unprecedented biomimetic transistor, highly sustainable and reliable soft electronic applications can be introduced.

and motion; they would revolutionize present prognosis methods by introducing fast, cheap, and noninvasive alternatives.^[3,5,8,13] Soft and flexible sensors can satisfy several mechanical requirements, including conformal attachment to the body, stretchability, and softness, giving greater sensing efficiency.^[3,4,6,8,10,14,15] However, devices with these properties are susceptible to mechanical/structural damage (e.g., cracks and scratches), which can result from the combined effect of their soft nature and incompatibility in mechanical stress with human skin. Inevitably, this leads to a lower durability, decreased life-time, and reduced performance in many cases.^[16–18] To address this issue, one can mimic biological systems by introducing a self-healing capability—a vital property for many organisms in nature—into flexible and soft devices, allowing the recovery of damages without external interventions.^[18–22]

Soft and flexible devices offer a wide spectrum of promising applications,^[1–12] e.g., epidermal sensors that can continuously monitor the health status of human body, including temperature, sweat,


Excellent progress in the development of new self-healing materials has been made in nonelectronic systems as well as in chemiresistors, supercapacitors, and electrochemical devices.^[22–24] Nevertheless, field effect transistors (FETs) with extractable multiparameters, offering considerable advantages as a sensor over other competing strategies by delivering a label-free response using a simple electronic readout setup that can be easily miniaturized by employing printed circuit technologies,^[25] has not yet been targeted. To prepare FETs, self-healing insulator (dielectric), conductive (electrodes), and semiconductive (channel) materials are required, with the latter being the more challenging. The difficulty of obtaining such material arises from the rigidity of semiconductors because of their conjugated and high crystalline structure, which is contradictory to the softness and high chain mobility of self-healing materials. Recently, Bao and co-workers have succeeded in synthesizing a healable semiconducting polymer based on 3,6-di(thiophen-2-yl)-2,5-dihydropyrrolo[3,4-c]pyrrole-1,4-dione repeating units and nonconjugated 2,6-pyridine dicarboxamide moieties with a μ_h of $\approx 1.4 \text{ cm}^2 \text{ V}^{-1} \text{ s}^{-1}$, $\approx 10^6$ on/off ratio, and high operating voltages up to -60 V . Nevertheless, the healing process needed solvent treatment or high temperatures for electrical and mechanical recovery with the limitation of self-healable damage size ($<100 \text{ nm}$ nanocracks) as well.^[26] Indeed,

M. Khatib, Dr. Y. Deng, Y. D. Horev, W. Saliba, Prof. H. Haick
The Department of Chemical Engineering
Technion – Israel Institute of Technology
Haifa 3200003, Israel
E-mail: hhossam@technion.ac.il

Dr. T.-P. Huynh
Laboratory of Physical Chemistry
Faculty of Science and Engineering
Åbo Akademi University
Porthaninkatu 3-5, 20500 Turku, Finland

Y. D. Horev, Prof. H. Haick
The Russell Berrie Nanotechnology Institute
Technion – Israel Institute of Technology
Haifa 3200003, Israel

Prof. W. Wu, Prof. H. Haick
School of Advanced Materials and Nanotechnology
Xidian University
Shaanxi 710126, P.R. China

 The ORCID identification number(s) for the author(s) of this article can be found under <https://doi.org/10.1002/sml.201803939>.

DOI: 10.1002/sml.201803939

developing a fully self-healable FET both in device morphology and function under room condition to ensure the long-term reliable work remains challenging.

Herein, an intrinsic and fully self-healing FET based carbon nanotubes (CNTs) with high electrical performances is fabricated by a facile approach. The FET's structural and electrical properties can remarkably be self-recovered in room condition after multiple cycles of micro-sized damage and even a complete cut of the device. Moreover, the sensing abilities of the reported self-healable FET, both for physical (e.g., temperature) or chemical (e.g., humidity) stimuli are demonstrated.

An intrinsic self-healing disulfide-containing poly(urea-urethane) (PUU) similar to previously reported polymers was used in this work.^[20,27–29] It is composed of two monomers, 4-aminophenyl disulfide (APDS) and poly(propylene glycol) tolylene 2,4-diisocyanate terminated (PPG-TDI, Figure S1, Supporting Information). The polymerization reaction was followed by Fourier transform infrared (FTIR) spectroscopy (see Figure S2, Supporting Information). PUU contains dynamic hydrogen and disulfide bonds which can break and recover under room conditions without any additional energy.^[29] The reversible nature of these bonds combined with the low glass transition temperature (T_g) of the polymer make it a very efficient self-healing material (Figure S3, Supporting Information). We found a good trade-off between the mechanical property and self-healing ability by investigating the influence of the ratio of APDS to PPG-TDI on these properties. We synthesized three different polymers with APDS to PPG-TDI mass ratios of 11:100, 12:100, and 13:100, termed PUU11, PUU12, and PUU13, respectively. The high ratio led to a very soft polymer that could not hold its shape under ambient conditions. At the ratio close to 10.5:100 (1:1 by molar) we obtained a mechanically strong polymer that undergoes small deformation under mechanical stress (Figure S4, Supporting Information). On the other hand, considering the self-healing ability, higher APDS content led to a higher self-healing ability as the polymer produced proved softer (Figure S4, Supporting Information). In contrast to the previous material, we had succeeded in obtaining a soluble self-healing viscoelastic elastomer, instead of a thermoset,^[29] with good mechanical properties, $\approx 1000\%$ strain, and ≈ 0.26 MPa tensile strength at the break point. For fabrication of the device, we used PUU12 as it showed the best combination between mechanical properties and self-healing ability (Figures S4 and S5, Supporting Information). Similar to many low T_g polymers/elastomers, PUU12 has very high electrical capacitance (Figure S6, Supporting Information), which could be attributed to the high-mobility of chains, the high polarity, and the existence of ionic impurities inside the polymeric structure, such as residues that had become incorporated during synthesis of the elastomer.^[30] PUU12 has a dielectric constant of about 17.5 and 12.3 at the frequency of 10 and 1000 Hz, respectively. It is noteworthy that PUU is a hygroscopic elastomer due to the hydrophilic nature of its propylene glycol monomer. In addition, the absorption of water, which behaves as a plasticizer, improves the softness of PUU as well as its self-healing ability. All the self-healing experiments shown here were done under ambient conditions unless otherwise stated ($\approx 70\%$ humidity). However, we also tested the effect of humidity on

the self-healing ability of PUU. As expected, the self-healing process is faster at higher humidity levels due to the increased softness (Figure S7, Supporting Information).

Top-contact bottom-gate transistors were fabricated by transfer printing (Figure 1a). On the one hand, this method is super-convenient with self-healing polymers because it enables easy transfer and great attachment of one layer on to another. On the other hand, this method allows fabrication of epidermis-like device on human skin with a strong attachment to the body (Figure 1a; see Videos S1 and S2, Supporting Information). For semiconductor preparation, CNTs were plastered to the surface of the PUU12 dielectric to obtain both semiconductivity and self-healing abilities (Figure 1b); the same strategy, but with conductive CNTs, used to prepare the electrodes. A representative self-healing transistor with 200 μm channel-length and 5000 μm channel-width was used to measure performance (Figure 1c). A typical output curve of the transistor, showing a good linear and saturated behavior, and a representative transfer curve, are depicted in Figure 1d,e. High on-current (I_{on}) of $\approx 30 \mu\text{A}$, μ_h of $\approx 10 \text{ cm}^2 \text{ V}^{-1} \text{ s}^{-1}$, and an average on/off ratio of $\approx 10^3$ were obtained, consistent with previously reported CNT transistor using the same semiconducting material.^[31] Histograms of transistors showing the statistical distribution of the I_{on} , μ_h , and on/off ratio are presented in Figure S8 in the Supporting Information. The high capacitance of PUU12 allowed the device to turn on at low gate biases (up to 6 V), which is highly desirable for wearable electronics.

To examine the potential for autonomic self-healing ability (i.e., self-healing without aid from any external trigger, e.g., temperature, organic solvent vapor, and light) of each part of the FET, the device was cut using a sharp blade and followed by monitoring its performance and structural recovery with time. At the beginning, the self-healing ability of the conductive CNT network embedded in PUU12 was examined. Figure 2a shows optical images of the healing process of structural damage after a blade-cut made perpendicular to the conduction pathway. This conductive film can recover from a drastic cut ($\approx 5 \mu\text{m}$ in width and $\approx 2 \mu\text{m}$ in depth) quickly and maintain good conductivity. The self-healing process has a typical behavior with time; a very sharp increase in the conductivity can be seen at the beginning of the recovery, which decreases with time to reach a plateau (Figure 2b,c). The fast-initial self-healing is probably due to shape recovery of the elastic polymer near the damaged area, but this fast process is followed by slow recovery that might be dominated mainly by the surface rearrangement and diffusion of the polymer chains. The regeneration of the conductive pathway of CNTs is attributed to their interaction with the mobile chains of the polymer, which, in turn, leads to the lateral movement of CNTs toward the damaged region, allowing the reconstruction of the continuous pathway.^[32,33] We later examined the effect of mechanical damage ($\approx 5 \mu\text{m}$ in width and $\approx 2 \mu\text{m}$ in depth cut) on each part of the FET's structure. Illustration images of the position of the damages made on each part of the FET are shown in Figure S9 in the Supporting Information. In the case of gate damage, gate modulation was stopped after the cut, preventing further increase in the drain current (Figure 2d). The behavior of the FET was almost totally recovered after 1 h. The gate electrode could heal several cuts with negligible change in performance (Figure 2e). On the other

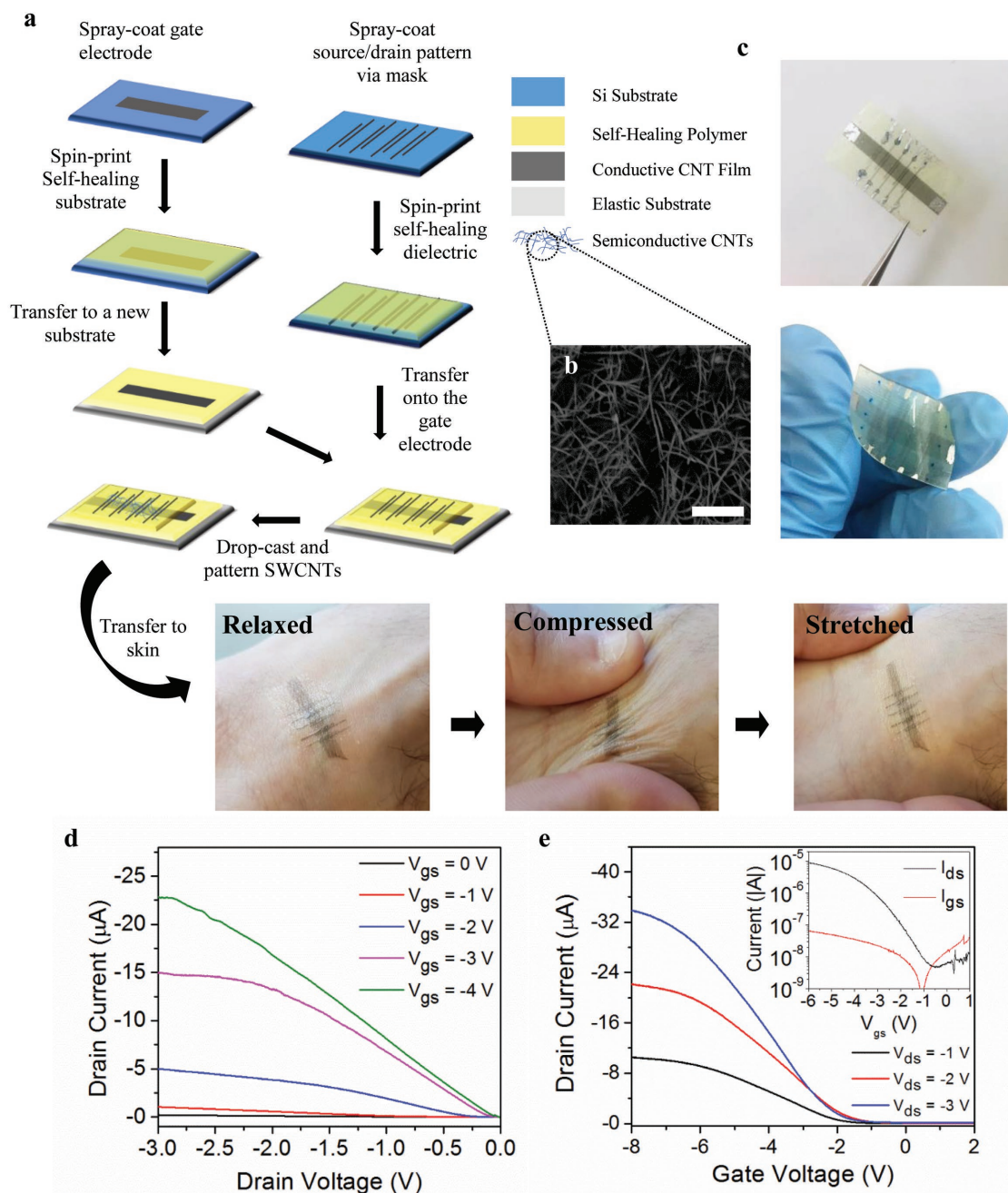


Figure 1. Fabrication process and device performance. a) Schematic illustration of the fabrication process for the self-healing transistor, and photographs of the self-healing electronic tattoo on skin. b) SEM images of the semiconductive CNT network printed on top of the dielectric layer. Scale bar, 1 μm . c) Photographs of a self-healing transistor array on PET flexible substrate (top) and an elastic substrate (bottom). d) Output characteristics of the self-healing CNT transistor, with gate voltages from 0 to -4 V in -1 V steps. e) Transfer characteristics of the device with drain voltage from -1 to -3 V. Inset, transfer curve at $V_{\text{d}} = -1\text{ V}$ (black line), and gate-leakage current in the same range (red line). The performances shown in (d) and (e) were obtained from the self-healing transistor printed on an elastic substrate (styrene-isoprene copolymer).

hand, the drain current was dramatically decreased ($< 10^{-10}\text{ A}$) immediately after source/drain (SD) electrode cut, and then started to increase back toward the initial value. The self-healing process took 1 h and the last value was lower than the original value (Figure 2f). Several cut cycles in the SD electrode could also be recovered. The initial cut caused the largest decrease in the drain current compared to subsequent damage (Figure 2g).

The difference between the self-healing of the SD electrodes and the gate electrode is originated from the different function of each part; for the gate, which is used to polarize the dielectric layer, its conductivity is less important to the performance of the whole devices. The existence of microcracks, which are not perfectly recovered, does not significantly interrupt with the polarization behavior, especially with high- k elastic dielectric

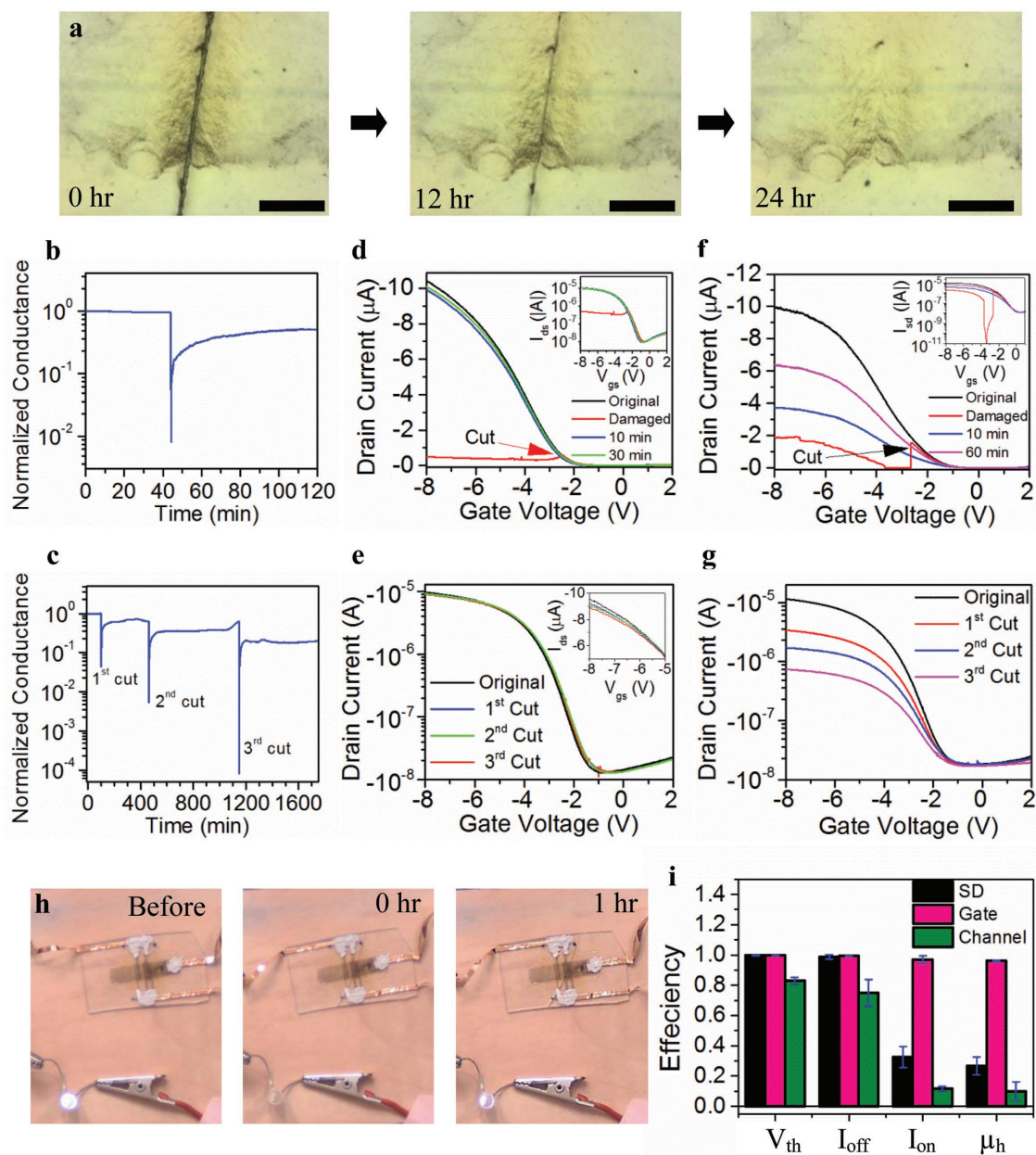


Figure 2. Self-healing ability of the transistor. a) Structural monitoring of the self-healing process of PUU12 at different times. Scale bar is 200 μm . b) Dynamicality of the self-healing process in CNT-PUU films. c) Recovery of several damage cycles in the CNT-PUU electrodes. Transfer curves showing d) the time-dependent healing of the gate (Inset shows logarithmic scale), and e) the ability of the gate to heal several cuts (Inset shows zoom-in on the high current regime). f) Transfer curves showing the time-dependent healing of the SD electrodes (Inset shows logarithmic scale). g) Transfer curves showing the ability to heal several cuts in the gate. h) Photographs displaying the self-healing ability of the transistor after being severed with a scissors. They show the intensity of LED that is driven by the self-healing transistor before the cut, directly after reconnecting the two cut parts, and 1 h after reconnection. i) Self-healing efficiencies of the three different damages based on four parameters: V_{th} , I_{on} , I_{off} , and μ_{h} . Efficiency was evaluated according to: $\varepsilon = (f_{\text{Healed}} - f_{\text{damaged}}) / (f_{\text{original}} - f_{\text{damaged}})$, where f is the characteristic parameter.

such as PUU12. The microcracks can be considered as additional capacitors that are connected in series. The additional in-series capacitors are equivalent to a capacitor with a thicker dielectric layer. Moreover, it is known that for many high- k elastomers the capacitance value is insensitive to the thickness of the dielectric.^[30] Therefore, we did not see any noticeable changes in the device performance after the recovery of the gate electrode. However, the conductivity of the SD electrodes

is very important as it directly affects the value of the drain current, and any unhealed part would increase the resistance and decrease the drain current, especially the I_{on} where low resistance electrodes are needed to deliver the maximum current. In contrast to the good recovery obtained with the gate and SD electrodes, similar damages in the channel were too destructive, leading to a decreased drain current by almost one order of magnitude after the healing process (Figures S10 and S11,

Supporting Information). This significant deterioration in performance can be explained by the lower self-healing ability of thinner layers. In the case of CNT semiconductive channel, with a thickness of <20 nm, micro-cuts are too large to be totally recovered because the damaged edges are highly deformed, preventing the complete reconnection of CNTs (Figure S12, Supporting Information). For real application, external cyclic stresses will lead to small microcracks but not such big-scale highly-deforming damages. The efficiency of self-healing was evaluated using four characteristic parameters: I_{on} , μ_{h} , off-current (I_{off}), and threshold voltage (V_{th}) (Figure 2i). Starting from gate damage, the healing efficiency of all parameters was very high (>98%), but damage in the SD showed lower self-healing ability. The μ_{h} and the I_{on} have decreased by a factor of 3, whereas the I_{off} and V_{th} had efficiently recovered to near their initial values. Regarding channel damage, as explained above, a cut was very destructive, resulting in low self-healing efficiencies, $\approx 10\%$ with respect to I_{on} and μ_{h} . The efficiencies of the I_{off} and V_{th} were also affected, but they remained relatively high (>75%). To produce more severe damage, the whole device was completely cut with scissors and its performance monitored

after the reconnection of the two parts. Unexpectedly, a transistor-like behavior was recovered after ≈ 24 h (Figure S13, Supporting Information). This also proved to be the case using a light emitting diode (LED) driven by the self-healing transistor. Figure 2h shows that directly after the reconnection there was no noticeable light intensity, but this gradually increased with time (see Video S3, Supporting Information).

The device performance was tested under uniaxial strain either parallel or perpendicular to the charge transport direction. First, the devices were conditioned by initial cycles of strain up to 50%, rendering them with minimal sensitivity/drain current in subsequent strains. Transfer curves were monitored under varying strain values and strain cycles (Figure 3a,b). Figure 3a displays the transfer curves of the transistor under different strain values from 0% to 50% before and after conditioning. The I_{off} , I_{on} , and μ_{h} decreased by up to $\approx 60\%$ with 50% strain (Figure 3c–e). The V_{th} slightly shifted to more negative values as the strain increased (Figure 3c–f), which might be explained by the small decrease in the capacitance as stretching leads to arranged polymer chains, decreased polarity, and lower content of water. After the first stretching cycle, the device became

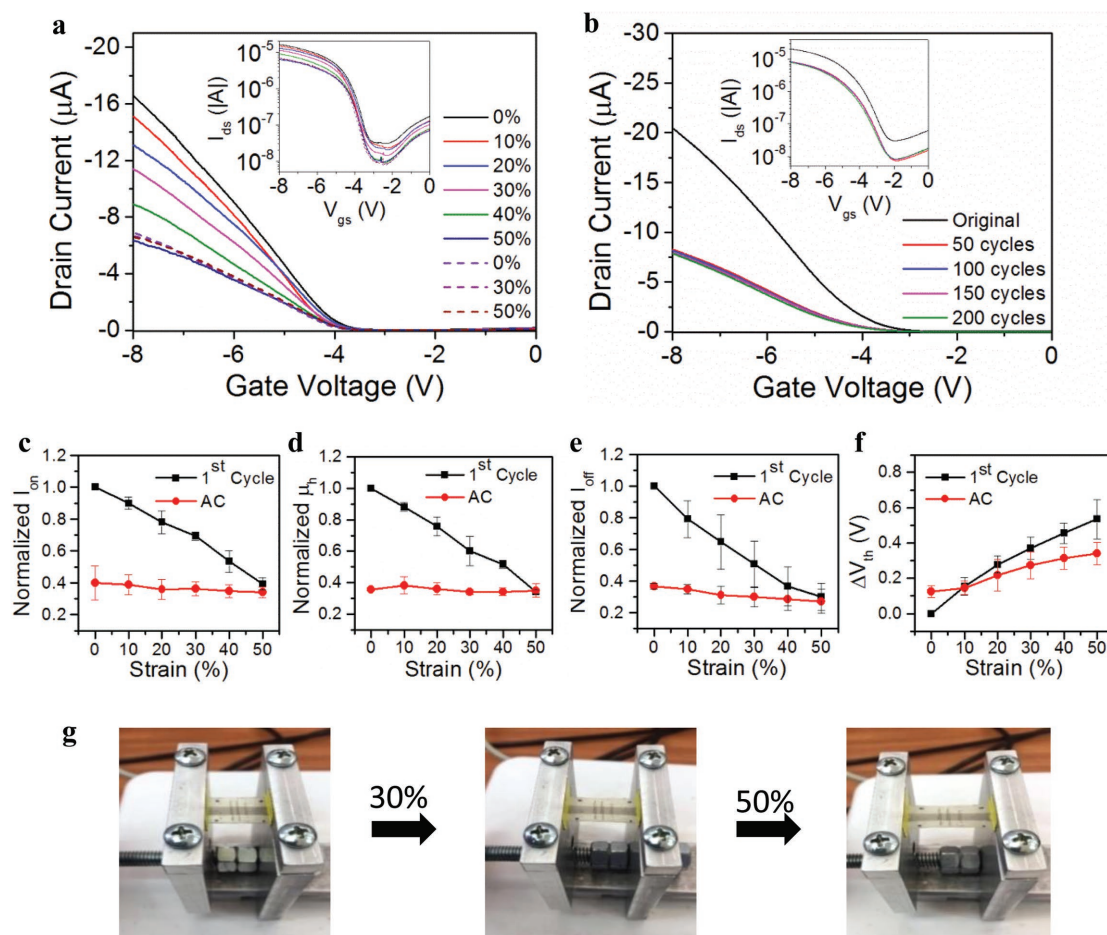


Figure 3. Strain-dependent properties of the self-healing device. a) Typical transfer characteristics ($V_{\text{D}} = -2.0$ V) of a the device under different tensile strains (from 0% to 50%) applied along the channel length direction; solid lines represent the first stretching cycle while dashed lines represent the second stretching cycle. b) Typical transfer characteristics ($V_{\text{D}} = -2.0$ V) of a the device after cycles of 50% strain. Insets show log-scale characteristics. Normalized electrical characteristics for stretched devices: c) I_{on} , d) μ_{h} e) I_{off} , and f) V_{th} . g) Photographs of a device at different strains applied along the channel length direction.

less sensitive to strains, with the changes in the I_{off} , I_{on} , and μ_{h} with strain becoming almost negligible. This behavior was noticed with CNT-based elastomers and it is attributed to the spring-like structure of CNTs obtained after the first cycle of stretching.^[34] However, the V_{th} maintained some sensitivity to strain that is caused by the decrease in capacitance with increasing strains, but it was lower compared to the original device (Figure 3c–f). Having both strain-dependent and strain-independent parameters is desirable for obtaining multifunctional devices that can simultaneously detect strain values and other stimuli, e.g., temperature and humidity, without the need for complicated data processing to separate the responses to each type of stimulus. Similar behavior was also observed with uniaxial strains perpendicular to the channel conduction pathway (Figure S14, Supporting Information). A fatigue test was subsequently performed by applying continuous strain relaxation cycles up to 50% strain. Figure 3b shows the transfer

curves of the FET after different numbers of strain. As seen in the figure, the FET exhibited a negligible change with increasing number of cycles after the conditioning process.

The self-healing FET is a multifunctional device that can be used for many applications, such as sensing temperature and humidity. Figure 4a shows the responses of the FET to temperatures from 0 to 60 °C. The sensitivity of the FET in lower temperatures was higher compared to high temperatures; the I_{on} and I_{off} had the biggest changes in lower temperatures (Figure 4b). This might be explained by the lower temperatures limiting polymer mobility/softness, which decreases the gate modulation ability and also the I_{on} . Similar effect was seen in the case of the V_{th} where higher temperatures lead to lower V_{th} values (Figure S15, Supporting Information). This sensing ability was conserved after the healing of a structural damage. Figure 4b compares the normalized responses of pristine and recovered sensors. In this case, mechanical damage affected all

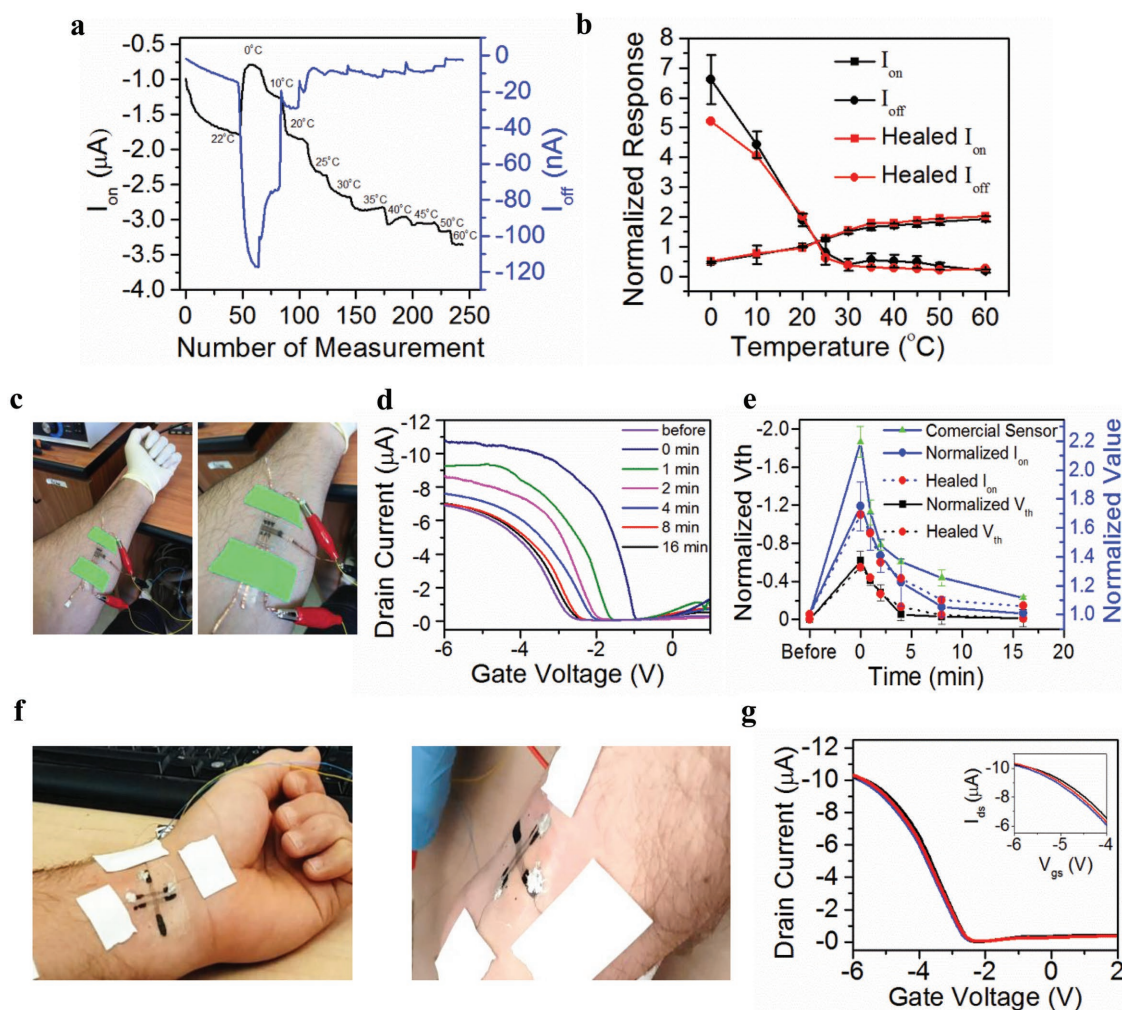


Figure 4. Transistor-based self-healing applications. a) Transistor sensitivity to different temperatures: Responses of I_{on} (black line) and I_{off} (blue line). b) Normalized responses of I_{on} and I_{off} before and after self-healing. Similar responses are obtained in both cases, indicating that the self-healing ability of the sensor is very efficient. c) Photographs of the epidermal humidity sensor mounted on the skin of the arm. d) Transfer curves obtained from the humidity epidermal sensor at different times after skin humidification. e) Normalized responses of I_{on} and V_{th} compared to the normalized response of a commercial sensor before and after self-healing. Damage has a negligible effect on the sensitivity of sensors that completed the healing process. f) Photographs of the epidermal self-healing skin tattoo during measurements. g) Performance of the self-healing transistor skin tattoo in different hand positions that lead to different strains on the skin tattoo. The different hand positions are presented in Figure S18 in the Supporting Information.

parts of the FET (Figure S16, Supporting Information), but the difference between the two cases was negligible.

Since the elasticity and the capacitance of PUU12 are highly affected by humidity, we have examined the potential of the developed FET to sense humidity values or hydration levels of the skin. Towards this end, we first tested the response of the device to different humidity values ranging from 0% to 100%. As expected, the devices showed lower V_{th} and higher I_{on} under higher humidity values (Figure S17, Supporting Information). In the second experiment we used the self-healing FET as an epidermal skin for humidity detection (Figure 4c). For the sake of comparison, we examined the performance of a commercial skin humidity sensor under the same experimental conditions. I_{on} and V_{th} were used to monitor the hydration of skin. Figure 4d presents the transfer curves obtained at different times after the application of lotion. The transistor shows lower V_{th} directly after the humidification, which decreases and slowly with time approaches the original value. Similar trend was seen with the I_{on} . Figure 4e gives the results of this experiment; same behavior was seen after self-healing of the sensor.

To demonstrate the final capability of this self-healing sensor we showed its application to the skin as an ultrathin tattoo ($\approx 3 \mu\text{m}$ thick), making it highly promising for future diagnostic applications (Figure 4f). The attachment of the sensor was only due to van der Waals interactions and without using any adhesives. The performance of the epidermal sensor was tested under different skin strains; the behavior was stable as very negligible changes being observed with different hand positions (Figure 4g; see Video S4, Supporting Information).

To summarize, we have introduced the first autonomic self-healing and stretchable FET using a self-healing PUU as a host matrix filled with conductive or semiconductive CNTs. The self-healing FET can recover several and varying degrees of mechanical damage ranging from microcracks to complete cut of the whole device by scissors. Moreover, the device can be repeatedly stretched for >200 cycles of up to 50% strain without a significant loss in its electrical properties. The self-healing and high stretchability of the device improve its lifetime as well as potentially enhancing its autonomic functionality. The transistor is demonstrated as a multifunctional sensor that detects temperature and humidity. In addition, the self-healing device can be applied as an ultrathin temporary tattoo to skin. This platform is very promising for in situ analysis of skin chemical and physical environments by modern epidermal applications that facilitate personalized and continuous physiological and clinical investigations. The reported self-healing transistor raises expectations that flexible and stretchable devices might one day become fully autonomic, thus increasing their lifetime and reliability in several applications, such as e-skin, wearable electronics, and hard-to-reach instruments. In addition, the integration of self-healing capability will increase sustainability of electronic systems leading to more environmentally friendly applications.

Supporting Information

Supporting Information is available from the Wiley Online Library or from the author.

Acknowledgements

An informed consent was obtained from Muhammad Khatib for using the developed patch on his skin.

Conflict of Interest

The authors declare no conflict of interest.

Keywords

carbon nanotubes, electronic tattoos, field-effect transistors, self-healing, stretchable

Received: September 22, 2018

Revised: November 22, 2018

Published online: December 12, 2018

- [1] A. Chortos, Z. Bao, *Mater. Today* **2014**, 17, 321.
- [2] Z. Liu, Z. S. Wu, S. Yang, R. Dong, X. Feng, K. Müllen, *Adv. Mater.* **2016**, 28, 2217.
- [3] D.-H. Kim, R. Ghaffari, N. Lu, J. A. Rogers, *Annu. Rev. Biomed. Eng.* **2012**, 14, 113.
- [4] M. J. Cima, *Nat. Biotechnol.* **2014**, 32, 642.
- [5] W. Gao, S. Emaminejad, H. Y. Y. Nyein, S. Challa, K. Chen, A. Peck, H. M. Fahad, H. Ota, H. Shiraki, D. Kiriya, *Nature* **2016**, 529, 509.
- [6] D.-H. Kim, N. Lu, R. Ma, Y.-S. Kim, R.-H. Kim, S. Wang, J. Wu, S. M. Won, H. Tao, A. Islam, *Science* **2011**, 333, 838.
- [7] C. Pang, C. Lee, K. Y. Suh, *J. Appl. Polym. Sci.* **2013**, 130, 1429.
- [8] D. Son, J. Lee, S. Qiao, R. Ghaffari, J. Kim, J. E. Lee, C. Song, S. J. Kim, D. J. Lee, S. W. Jun, *Nat. Nanotechnol.* **2014**, 9, 397.
- [9] M. Stoppa, A. Chiolerio, *Sensors* **2014**, 14, 11957.
- [10] R. C. Webb, A. P. Bonifas, A. Behnaz, Y. Zhang, K. J. Yu, H. Cheng, M. Shi, Z. Bian, Z. Liu, Y.-S. Kim, *Nat. Mater.* **2013**, 12, 938.
- [11] W. Zeng, L. Shu, Q. Li, S. Chen, F. Wang, X. M. Tao, *Adv. Mater.* **2014**, 26, 5310.
- [12] S. Xu, Y. Zhang, L. Jia, K. E. Mathewson, K.-I. Jang, J. Kim, H. Fu, X. Huang, P. Chava, R. Wang, *Science* **2014**, 344, 70.
- [13] Z. Sonner, E. Wilder, J. Heikenfeld, G. Kasting, F. Beyette, D. Swaile, F. Sherman, J. Joyce, J. Hagen, N. Kelley-Loughnane, *Biomicrofluidics* **2015**, 9, 031301.
- [14] S. S. Lobodzinski, M. M. Laks, *Cardiol. J.* **2012**, 19, 210.
- [15] D.-H. Kim, J. Viventi, J. J. Amsden, J. Xiao, L. Vigeland, Y.-S. Kim, J. A. Blanco, B. Panilaitis, E. S. Frechette, D. Contreras, *Nat. Mater.* **2010**, 9, 511.
- [16] X. Yang, C. An, S. Liu, T. Cheng, V. Bunpetch, Y. Liu, S. Dong, S. Li, X. Zou, T. Li, *Adv. Healthcare Mater.* **2018**, 7, 1701014.
- [17] R. F. Shepherd, F. Ilievski, W. Choi, S. A. Morin, A. A. Stokes, A. D. Mazzeo, X. Chen, M. Wang, G. M. Whitesides, *Proc. Natl. Acad. Sci. U. S. A.* **2011**, 108, 20400.
- [18] B. C. Tee, C. Wang, R. Allen, Z. Bao, *Nat. Nanotechnol.* **2012**, 7, 825.
- [19] S. R. White, N. Sottos, P. Geubelle, J. Moore, M. R. Kessler, S. Sriram, E. Brown, S. Viswanathan, *Nature* **2001**, 409, 794.
- [20] T. P. Huynh, H. Haick, *Adv. Mater.* **2016**, 28, 138.
- [21] C. Wang, H. Wu, Z. Chen, M. T. McDowell, Y. Cui, Z. Bao, *Nat. Chem.* **2013**, 5, 1042.
- [22] S. J. Benight, C. Wang, J. B. Tok, Z. Bao, *Prog. Polym. Sci.* **2013**, 38, 1961.
- [23] T. P. Huynh, P. Sonar, H. Haick, *Adv. Mater.* **2017**, 29, 1604973.
- [24] J. Li, L. Geng, G. Wang, H. Chu, H. Wei, *Chem. Mater.* **2017**, 29, 8932.

- [25] L. Torsi, M. Magliulo, K. Manoli, G. Palazzo, *Chem. Soc. Rev.* **2013**, 42, 8612.
- [26] J. Y. Oh, S. Rondeau-Gagné, Y.-C. Chiu, A. Chortos, F. Lissel, G.-J. N. Wang, B. C. Schroeder, T. Kurosawa, J. Lopez, T. Katsumata, *Nature*. **2016**, 539, 411.
- [27] T. P. Huynh, M. Khatib, R. Srour, M. Plotkin, W. Wu, R. Vishinkin, N. Hayek, H. Jin, O. M. Gazit, H. Haick, *Adv. Mater. Technol.* **2016**, 1, 1600187.
- [28] H. Jin, T.-P. Huynh, H. Haick, *Nano Lett.* **2016**, 16, 4194.
- [29] A. Rekondo, R. Martin, A. R. de Luzuriaga, G. Cabañero, H. J. Grande, I. Odriozola, *Mater. Horiz.* **2014**, 1, 237.
- [30] D. Kong, R. Pfattner, A. Chortos, C. Lu, A. C. Hinckley, C. Wang, W. Y. Lee, J. W. Chung, Z. Bao, *Adv. Funct. Mater.* **2016**, 26, 4680.
- [31] J. Liang, L. Li, D. Chen, T. Hajagos, Z. Ren, S.-Y. Chou, W. Hu, Q. Pei, *Nat. Commun.* **2015**, 6, 7647.
- [32] H. Wang, B. Zhu, W. Jiang, Y. Yang, W. R. Leow, H. Wang, X. Chen, *Adv. Mater.* **2014**, 26, 3638.
- [33] D. Son, J. Kang, O. Vardoulis, Y. Kim, N. Matsuhisa, J. Y. Oh, J. W. To, J. Mun, T. Katsumata, Y. Liu, *Nat. Nanotechnol.* **2018**, 13, 1057.
- [34] D. J. Lipomi, M. Vosgueritchian, B. C. Tee, S. L. Hellstrom, J. A. Lee, C. H. Fox, Z. Bao, *Nat. Nanotechnol.* **2011**, 6, 788.